STEM CELLS AND DEVELOPMENT
Volume 23, Number 12, 2014

DOI: 10.1089/scd.2013.0510

Isolation and Transplantation of Corneal Endothelial Cell–Like Cells Derived from In-Vitro-Differentiated Human Embryonic Stem Cells

Kai Zhang,[1,2] Kunpeng Pang,[1] and Xinyi Wu[1]

The maintenance of corneal dehydration and transparency depends on barrier and pump functions of corneal endothelial cells (CECs). The human CECs have no proliferation capacity in vivo and the ability to divide in vitro under culture conditions is dramatically limited. Thus, the acquisition of massive cells analogous to normal human CECs is extremely necessary whether from the perspective of cellular basic research or from clinical applications. Here we report the derivation of CEC-like cells from human embryonic stem cells (hESCs) through the periocular mesenchymal precursor (POMP) phase. Using the transwell coculture system of hESCs with differentiated human corneal stromal cells, we induced hESCs to differentiate into POMPs. Then, CEC-like cells were derived from POMPs with lens epithelial cell–conditioned medium. Within 1 week, CEC-like cells that expressed the corneal endothelium (CE) differentiation marker N-cadherin and transcription factors FoxC1 and Pitx2 were detectable. Fluorescence-activated cell sorting (FACS)–based isolation of the N-cadherin/vimentin dual-positive population enriches for CEC-like cells. The isolated CEC-like cells were labeled with carboxyfluorescein diacetate, succinimidyl ester (CFDA SE) and seeded onto posterior acellular porcine corneal matrix lamellae to construct the CEC-like cell sheets. Pump function parameters of the CEC-like cell sheets approximated those of human donor corneas. Importantly, when the CEC-like cell sheets were transplanted into the eyes of rabbit CE dysfunction models, the corneal transparency was restored gradually. In conclusion, CEC-like cells derived from hESCs displayed characteristics of native human CECs. This renewable source of human CECs offers massive cells for further studies of human CEC biological characteristics and potential applications of replacement therapies as substitution for donor CECs in the future.

Introduction

EMBRYONIC STEM CELLS are pluripotent cells derived from the inner cell mass of the blastocyst that can be maintained in culture for an extended period of time without losing differentiation potential. The successful isolation of human embryonic stem cells (hESCs) has raised the hope that may provide a potentially unlimited supply of cells that may be directed to differentiate into all cell types within the body and used in regenerative medicine for tissue and cell replacement therapies [1,2]. However, directed differentiation of hESCs into specific tissue types poses a formidable challenge because the growth factors and three-dimensional signals that control hESC differentiation have remained elusive. Protocols are currently available for only a few cell types, mostly of neural identity [3–7] and the paraxial mesoderm derivatives [8–11], and the differentiation into the cell types derived from the periocular mesenchymal precursors (POMPs) has not been reported. One of the cell types derived from the POMPs is corneal endothelial cells (CECs) [12].

The corneal endothelium (CE) consists of a single layer of regularly arranged hexagonal cells (ie, CECs) that separate the corneal stroma from the aqueous humor of the anterior chamber. Corneal transparency is maintained by regulation of stromal hydration through the barrier and pump functions of the CECs. Human CECs do not normally divide in vivo at a rate sufficient to replace dead or injured cells [13–16] and if the density of endothelial cells is too low, then barrier function is lost and more fluid enters the cornea resulting in corneal edema, development of bullous keratopathy, and loss of visual acuity, characteristic of human CE dysfunction. Replacing the diseased or injured CECs with healthy donor CE via penetrating keratoplasty or endothelial keratoplasty is the solely effective method for treating human CE dysfunction to date. Given the fact that corneas that are

[1]Department of Ophthalmology, Qilu Hospital, Shandong University, Jinan, People's Republic of China.
[2]The Key Laboratory of Cardiovascular Remodeling and Function Research, Chinese Ministry of Education and Chinese Ministry of Health, Qilu Hospital, Shandong University, Jinan, People's Republic of China.

considered to be acceptable for transplantation are becoming less available worldwide [17] and the aging of the ''baby boomer'' generation will bring a greater need for donor corneas to restore corneal clarity lost due to CE dysfunction, it is imperative for us to obtain sufficient number of cells analogous to human CECs that can be used for cell biological research and replacement therapies.

In this study, we present techniques for the generation and purification of CEC-like cells with phenotypic, genetic, and functional characteristics of normal human CECs from hESCs. Our isolation method for CEC-like cells is the first example, to our knowledge, of efficiently deriving structures of POMPs from hESCs, and further highlights the potential of hESCs for basic biology and regenerative medicine.

Materials and Methods

Cell culture

The hESC cell line was generously provided by Center of Reproductive Medicine, Shandong University [18], and cultured on irradiated mouse embryonic fibroblast feeder layers. The hESC culture medium consisted of 80% Dulbecco's modified Eagle's medium (DMEM)/F12 (1:1), 20% knockout serum replacement, 200 mM L-glutamine, 10 mM nonessential amino acids (all obtained from Invitrogen), 14.3 M β-mercaptoethanol (Sigma), and 8 ng/mL basic fibroblast growth factor (bFGF; Invitrogen). Cell cultures were incubated at 37°C in a humidified atmosphere containing 5% CO_2 with medium changes every day and manually passaged once per week. To induce CEC-like cell differentiation, embryoid bodies (EBs) were formed and cultured in suspension for 7 days with hESC growth medium in low-attachment culture dishes.

Corneas were obtained from the Eye Tissue Bank of Shandong Province, China, at 7–8 days postmortem. The age of the donors was 35–60 years. The basal medium (BM) contained DMEM/F12 supplemented with B27 (Invitrogen), 20 ng/mL epidermal growth factor (Sigma), and 40 ng/mL bFGF. The corneal stroma deprived of epithelial and endothelial cells was cut into small pieces ~10 mm in diameter, which were digested into single cells with 0.02% collagenase (Sigma). To promote fibroblast differentiation, 10% fetal bovine serum (FBS; Invitrogen) was added to BM to form corneal fibroblast differentiation medium (FM). The isolated human corneal stromal cells (hCSCs) were plated at 1,800/cm^2 onto 0.4-μm-pore transwell inserts (Corning) and cultured in FM.

Preparation of lens epithelial cell–conditioned medium and derivation of CEC-like cells from hESCs

SV-40-transformed human lens epithelial cells were obtained from the Shanghai ay Biological Technology Co. Ltd. and cultured in DMEM/F12 containing 20% FBS. Lens epithelial cell–conditioned medium (LECCM) was derived by collecting the medium from these cultured cells at 70%–90% confluence every 12 h. The collected medium was filtered (0.22 mm) to remove dead cells and stored at −80°C to preserve its biological activity. LECCM was mixed with FM at a ratio of 3:1 as the CEC differentiation medium (EM).

Approximately 80 EBs per well were plated onto 10 μg/mL fibronectin–10 μg/mL laminin–10 mg/mL heparan sulfate–precoated, 24-mm-diameter glass coverslips in wells of a six-well tissue culture plate and cultured in BM for 2 days. Subsequently, the hCSCs on transwell inserts were added to the six-well plates and cocultured with the plated EBs in FM for an additional 5 days with the medium changes every 2 days. Then, the medium was changed from FM to EM and culturing was continued until 2 weeks.

Immunofluorescent staining

Cells were fixed with 4% paraformaldehyde for 30 min and incubated in phosphate-buffered saline with 0.5% Triton X-100 (PBST) containing 1% goat serum albumin for 1 h. Primary antibodies were mouse anti-OCT-4 (1:100; Santa Cruz), mouse anti-CD73 (1:500; BD Biosciences), rabbit anti-FoxC1 (1:200; Abcam), rabbit anti-PitX2 (1:200; Abcam), mouse anti-N-cadherin (1:500; BD Biosciences), rabbit anti-vimentin (1:200; Abcam), rabbit anti-zonula occludens-1 (ZO-1, 1:100; Zymed Laboratory, Invitrogen), and mouse anti-Na^+/K^+ ATPase α1 (1:50; Santa Cruz). Cells were rinsed in PBST and then incubated with the primary antibodies for 1 h at 37°C or overnight at 4°C. Secondary antibodies (1:100; all obtained from Beijing Zhongshan) coupled to FITC or TRITC were then applied for detection, and cells were stained with 4′,6-diamidino-2-phenylindole (DAPI) to visualize nuclei. In negative controls, primary antibodies were substituted by PBS. Fluorescence was observed by using a fluorescence microscope (models BH2-RFL-T3 and BX50; Olympus).

Fluorescence-activated cell sorting analysis and purification

hESC colonies were dissociated by incubating them for 5 min at 37°C in Accumax (Chemicon) and gently triturated into single cells. The dissociated hESCs were fixed and permeabilized with Cytofix/Cytoperm Kit (BD Biosciences Pharmingen) following manufacturer's instruction. Cells were incubated with the primary antibody for CD73 at 37°C for 20 min, and then washed three times with PBS. Goat anti-mouse IgG antibodies conjugated with FITC were used as secondary antibodies. For N-cadherin and vimentin double staining, the cells were stained with N-cadherin first, followed by goat anti-mouse IgG FITC, and then the vimentin and goat anti-rabbit IgG TRITC. Cells were washed with PBS before analysis using a fluorescence-activated cell sorting (FACS) Calibur (BD Biosciences). In negative controls, primary antibodies were substituted by PBS. Cell isolation was conducted on an FACS Vantage or FACS Aria (BD Biosciences). Compensation for FITC and TRITC was performed using compensation beads (BD Pharmingen). Analysis was done using the Flow-Jo program (Tree Star). Positive and negative gates were determined using IgG-stained and unstained controls.

Western blotting

Total protein of POMPs and CEC-like cells was extracted, respectively, using 1% radio-immunoprecipitation assay lysis buffer (Beyotime) and quantified with bicinchoninic acid protein assay kit (Beyotime). Protein was loaded onto a 10%

sodium dodecyl sulfate–polyacrylamide gel electrophoresis, electrophoresed, and then transferred to a polyvinylidenedifluoride membrane (Millipore). Membranes were blocked with 5% nonfat dried milk overnight at 4°C, and then washed three times with TBST, and incubated with primary antibody against Na^+/K^+ ATPase α1 (1:2,000; Santa Cruz) and β1 (1:1,000; Santa Cruz) and β-actin (1:500; obtained from Beijing Zhongshan) overnight at 4°C. After immunoblotting with secondary antibodies (1:5,000; Beyotime) at room temperature for 1 h, the protein was detected with an enhanced chemiluminescence reagent (Millipore).

Real-time reverse transcription polymerase chain reaction

Total RNA was extracted from isolated POMPs and CEC-like cells by lysis in 1 mL TRIZOL (Invitrogen) followed by one-step chloroform-isopropanol extraction as described in the manufacturer's protocol. About 2.0 μg of total RNA was reverse transcribed into complementary DNA (cDNA) by incubation with 4 μL 5×RT buffer, 1 μL RT enzyme mix, and 2 μL primer mix in 10 μL reaction solution (TOYOBO) at 37°C for 15 min. As a template for the polymerase chain reaction (PCR), 1 μL of cDNA was mixed with 10 μL of SYBR premix ex taq (TOYOBO), 1 μL each of specific forward and reverse primers, and 8 μL RNase-Free water. The primer sequences were designed by Primer Premier 5 as follows: Na^+/K^+ ATPase α1, forward 5′-TGTGTTCCT GGGTGTGTCTTTC-3′, reverse 5′-CCATGCGTTTTGC AGTAAGTG-3′; and Na^+/K^+ ATPase β1, forward 5′-GGA ACGAAGTATAACCCAAATG-3′, reverse 5′-AGGAAAA CCAGCGTAATCAC-3′. Specific primers for the GAPDH gene were used as controls. Real-time reverse transcription–polymerase chain reaction (RT-PCR) was run in duplicate using the Light Cycler (Roche) at 95°C for 30 s, followed by 45 cycles of 95°C for 5 s, 60°C for 30 s, 95°C for 15 s, 55°C for 30 s, and finally at 95°C for 15 s. For normalization of gene expression levels, the ratio of gene-to-GAPDH (housekeeping gene) was calculated. Light Cycler software and the Light Cycler Relative Quantification software (Roche) were used to analyze the data.

Preparation of posterior acellular porcine corneal matrix lamellae and construction of CEC-like cell sheets

Decellularization of porcine corneas was implemented according to the previous protocols in our lab [19,20]. A 1.0-mm-thick, 8.0-mm-diameter APCM lamella containing posterior stromal collagen and Descemet's membrane [ie, posterior acellular porcine corneal matrix (PAPCM) lamella] was prepared using a scalpel under a dissecting microscope. PAPCM lamellae were washed three times in sterile PBS supplemented with 200 U/mL penicillin and 200 U/mL streptomycin for 3 h, freeze-dried at −20°C for 12 h, air-dried at room temperature for 3 h in a biological safety cabinet, and stored at −20°C before use. All steps were conducted under sterile conditions.

PAPCM lamellae were soaked in EM at 37°C for 24 h and isolated CEC-like cells were labeled with a kind of fluorescent dye called carboxyfluorescein diacetate, succinimidyl ester (CFDA SE; Beyotime) before construction of CEC-like cell sheets. Subsequently PAPCM lamellae were placed in individual wells of 96-well plates with the denuded Descemet's membrane facing up and CEC-like cells in 100 μL were gently seeded on the surface of Descemet's membrane at a density of 2×10^5 cells/mm^2 for each PAPCM lamella, allowing to adhere for 4 h before completely immerging in EM. These PAPCM lamellae bearing CEC-like cells (ie, CEC-like cell sheets) were cultured for 2 weeks.

Morphological and histological analyses of PAPCM lamellae and CEC-like cell sheets

The gross views of a PAPCM lamella before being freeze/air-dried and after soaking in sterile glycerol for 1 h were observed, respectively, using a surgery microscope (Zeiss). The signal of CFDA SE was checked in 10 CEC-like cell sheets after 2 weeks of culture under a fluorescence microscope. The details of Descemet's membrane side were observed and the number of cells in a 0.1-mm^2 area was counted at three different sites in the 10 CEC-like cell sheets—the surface of Descemet's membrane of which had been stained with trypan blue and alizarin S. Cell density was expressed as mean of cell number per mm^2 ± SD. For histological examination, PAPCM lamellae and CEC-like cell sheets were fixed in 10% formalin and processed for paraffin embedding. Five micrometer sections were cut and stained with hematoxylin and eosin (H&E).

Measurement of pump function of the CEC-like cell sheet in vitro

Pump functions of three CEC-like cell sheets were measured, with some modifications, in a Ussing chamber (Model EM-LVSYS-4; Physiologic Instruments) as reported previously [21,22]. The epithelium of donor corneas was scraped mechanically. The donor corneas ($n=3$), PAPCM lamellae ($n=3$), and CEC-like cell sheets ($n=3$) were mounted in the Ussing chamber. Corneas were incubated in Ringer solution containing (in mM) NaCl, 117.5; $NaHCO_2$, 24; KCl, 4; Na_2HPO_4, 1; $MgSO_4$, 1; glucose, 4.45; reduced glutathione, 1; and $CaCl_2$, 2.54, and bubbled with a 5% CO_2, 7% O_2, and 88% N_2 gas mixture to pH 7.38. After steady state levels of the potential difference and short-circuit current were reached, ouabain (0.1 mM), a Na^+/K^+ ATPase inhibitor, was added to the chamber, and the potential differences and short-circuit current were measured again. The software for data acquisition is Acquire & Analyze rev II.

Transplantation of CEC-like cells into rabbits receiving Descemet's membrane striping

This research was approved by experimentation committee of Shandong University Qilu Hospital. Treatment was in accordance with the ARVO Statement for the Use of Animals in Ophthalmic and Vision Research. Male adult New Zealand White rabbits, weighing 1.5–2.0 kg, were anesthetized intravenously with 1% pentobarbital sodium (40–50 mg/kg) and topically with oxybuprocaine hydrochloride. After disinfection and sterile draping of the operation site, a 4-mm sclerocorneal incision centered at 12 o'clock was made with a slit knife, and a viscoelastic agent

(Healon; Amersham Pharmacia Biotech AB) was infused into the anterior chamber. The procedure for stripping central Descemet's membrane and transplanting the sheet was described in the ''Results'' section. Finally, the sclerocorneal wound was closed with two interrupted 10-0 nylon sutures (Alcon) and dexamethasone-tobramycin ointment (Santen) was instilled into conjunctiva sac immediately.

Twenty rabbits were selected and randomly divided into two groups: the CEC-like cells (rabbits with Descemet's membrane striping and CEC-like cell sheet transplantation, $n=10$) and PAPCM lamellae (rabbits with Descemet's membrane striping and PAPCM lamella transplantation, $n=10$). After transplantation, dexamethasone-tobramycin drops (Santen) were applied to the operative eye three times daily during the follow-up period.

Clinical observations

Each surgical eye ($n=20$) was photographed with a slit-lamp microscope (Zeiss) 1, 3, 5, 7, 14, 21, and 28 days after surgery. Central corneal thickness was measured 1, 3, 5, 7, 14, 21, and 28 days after surgery using a visante OCT (Model CA94568; Carl Zeiss Meditec, Inc.). Images of CEC-like cells were taken and analyzed by specular microscope (Model SP-2000P; Topcon Corporation) or confocal microscopy through focusing (HRT-II; Heidelberg Engineering). An average of three readings was taken and results were reported as average value $\pm$ SD.

Evaluation of CEC-like cells and histological examination

Twenty-eight days after transplantation, the rabbits, under deep anesthesia, were sacrificed by an intravenous overdose of pentobarbital sodium. Postoperative eyes were removed and the corneas were viewed as whole-mounts under a fluorescence microscope to examine CFDA SE fluorescence. Then, these corneas were bisected. One half of the divided cornea was double stained with alizarin red S and trypan blue to show cell survival and borders. The other half was fixed and 5-μm sections were subjected to H&E staining. Photos were taken with an inverted light microscope and the images were saved to a computer.

Statistics

SPSS 17.0 was used and the comparisons of the corneal thickness among the two groups were made using Student's *t*-test. The level of significance was set at $P<0.05$.

Results

The differentiation of hESCs into POMPs via transwell coculture with differentiated hCSCs

It is known that hCSCs originate from POMPs during development of the cornea and have the capacity to differentiate into fibroblasts both in vitro and in vivo [23,24]. Therefore, we postulated that exposing hESCs to hCSCs undergoing fibroblastic differentiation would stimulate differentiation of hESCs along the periocular mesenchymal lineage. In this study, hESC-derived EBs were cocultured with hCSCs undergoing fibroblastic differentiation in the transwell coculture system.

hESCs grown on mouse feeders displayed a typical aggregate morphology (Fig. 1A) and stained positively for OCT-4 (Fig. 1B), a marker for undifferentiated ESCs [25]. The differentiated hCSCs displayed a spindle-like shape (Fig. 1C), characteristic of human corneal fibroblasts, and reached confluency by 7 days. Immunofluorescent staining showed that vimentin was abundantly distributed in the cell plasma (Fig. 1D).

Prior to coculturing with hCSCs, the hESC aggregates were mechanically isolated from the mouse feeders and formed into EBs that were held in suspension for 7 days (Fig. 1E). Previous research indicated that the substrates fibronectin, laminin, and heparan sulfate 6 were permissive of emigrating of neural crest cells [26] from which POMPs were derived and induction of CEC-like cells [27–29]. Therefore, the hESC-derived EBs were plated onto fibronectin-laminin-heparan sulfate 6–coated plates before coculturing with hCSCs. After 5 days of coculture, the plated EBs had generated an outgrowth of migratory cells displaying an elongated spindle-like shape (Fig. 1G). Most emigrating cells coexpressed CD73 and FoxC1 (Fig. 1F, H), a combination of markers that is characteristic of POMPs. FACS indicated that the percentage of POMPs increased rapidly during the first few days of coculture and subsequently declined with prolonged time of culture (Fig. 1I).

The derivation of CEC-like cells from POMPs

FACS revealed that the number of POMPs ascended to the peak around day 5 after coculture (Fig. 1I). Hence, we selected the day 5 as the time point when the culture medium was changed from FM to EM and recorded the time as 0 day. During eye embroygenesis, the lens is critical for the formation of anterior segment and deletion of it leads to multiple anterior chamber defects including the absence of CECs [30–34]. In vitro, lens epithelial cell–derived medium (LECDM) was used to alter the phenotype of human umbilical cord blood mesenchymal stem cells (UCB-MSCs) toward that of human CECs by mimicking the effect of lens in embroygenesis [35]. Therefore, in this study, the EM consisted of LECDM and FM and the optimized ratio of them was 3:1 determined by preliminary experiments. Under the EM conditions, some POMPs at the periphery of plated EBs appeared morphological changes from elongated spindle-like shapes to hexagonal and pentagonal morphologies on day 3 (Fig. 2A, day 3) and the number of these cells continued to increase (Fig. 2A, day 7). On day 14 the majority of POMPs displayed hexagonal and pentagonal shapes and formed an endothelial monolayer (Fig. 2A, day 14).

To identify populations of putative CECs in our differentiating hESC cultures, we assayed expression of CEC-relative markers by immunostaining. During mammalian eye development, including human, FoxC1 is an important transcription factor which mutation will lead to severe anterior eye segment anomaly, such as the absence of CE [36,37]. FoxC1 is expressed initially in the POMPs and at later stages restricted to the forming corneal stroma and endothelium and prospective structures of trabecular meshwork [38]. Immunostaining results demonstrated that the majority of emigrating cells expressed FoxC1 in the nucleus before exposure to EM (Fig. 1F, H) and 5 days after exposure to EM (data not shown). PitX2 is another kind of

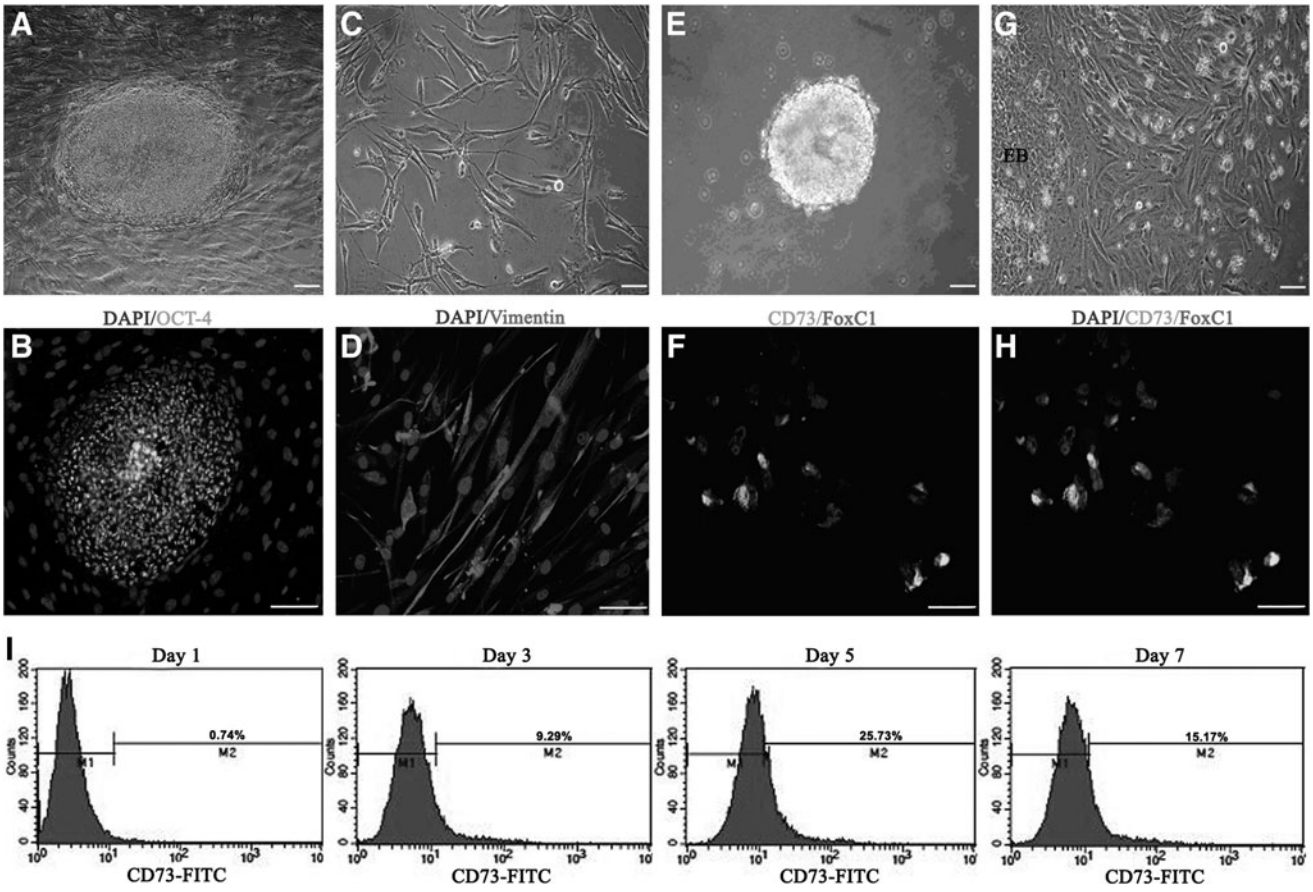

FIG. 1. Human embryonic stem cells (hESCs) differentiated into periocular mesenchymal precursors (POMPs) when cocultured with differentiated human corneal stromal cells (hCSCs). **(A)** hESC colonies grew on irradiated mouse embryonic fibroblast feeder layers. **(B)** The hESC aggregate was positive for OCT-4. The mouse embryonic fibroblast cells only stained for 4′,6-diamidino-2-phenylindole (DAPI) in the nuclei. **(C)** The differentiated hCSCs displayed a spindle-like shape, characteristic of corneal fibroblast cells. **(D)** The differentiated hCSCs showed high expression of vimentin. **(E)** The hESC-derived embryoid bodies (EBs) formed in suspension under feeder-free conditions on day 7. **(G)** Differentiating cells with morphology typical of mesenchymal lineage migrated out of an adherent EB after 5 days of coculture with differentiated hCSCs. **(F, H)** The majority of emigrating cells coexpressed CD73 and FoxC1, indicative of POMPs. **(I)** Analysis of EB-derived $CD73^+$ cells by fluorescence-activated cell sorting (FACS). $CD73^+$ cells appeared as early as day 1 of the coculture period, and the level of $CD73^+$ increased dramatically from day 3 to 5. M1: CD73-negative cells; M2: CD73-positive cells. Scale bars = 20 μm.

transcription factor analogous to FoxC1 [39]. The expression of PitX2 in the emigrating cells was similar to FoxC1 (data not shown). N-cadherin identified as cell–cell adherence protein is expressed in the developing CECs [40]. Vimentin is a kind of intermediate filament protein native to normal human CECs, localizing in the cytoplasm [41]. Therefore, it is reasonable to regard the cells coexpressing of N-cadherin and vimentin as CEC-like cells. Two weeks after exposure to EM, the coexpressing of N-cadherin and vimentin was found in the emigrating cells distant from the plated EBs (Fig. 2B).

The isolation and characterization of CEC-like cells

To purify and further characterize putative CECs derived from hESCs, we performed FACS to isolate N-cadherin/vimentin dual-positive cells in our bulk cultures. As shown in Fig. 2C, the percentage of CEC-like cells increased slowly after exposure to EM until day 14. We prolonged the induction time from 14 to 21 days; no increase of percentage of CEC-like cells was observed. Figure 2A showed the morphological changes of POMPs toward CECs under the EM conditions. To further demonstrate the differentiation to CECs, the western blotting and RT-PCR were performed to evaluate the expression of sodium-potassium pump Na^+/K^+ ATPase, an important functional protein of human CECs, in the isolated POMPs and CEC-like cells. The results showed the upregulation of Na^+/K^+ ATPase α1 and β1 subunits between POMPs and CEC-like cells (Fig. 3C, D).

Next, we proceeded to test whether the biological features of isolated CEC-like cells were comparative to those of normal human CECs after culturing on plates and the CEC-related functional proteins, sodium-potassium pump Na^+/K^+ ATPase and tight junction protein ZO-1, were expressed in these amplified cells. As shown in Fig. 3A, the isolated CEC-like cells adhered to the culture plates and grown to form a monolayer of hexagonal and pentagonal cells through 7 days of culture. When the culturing time was

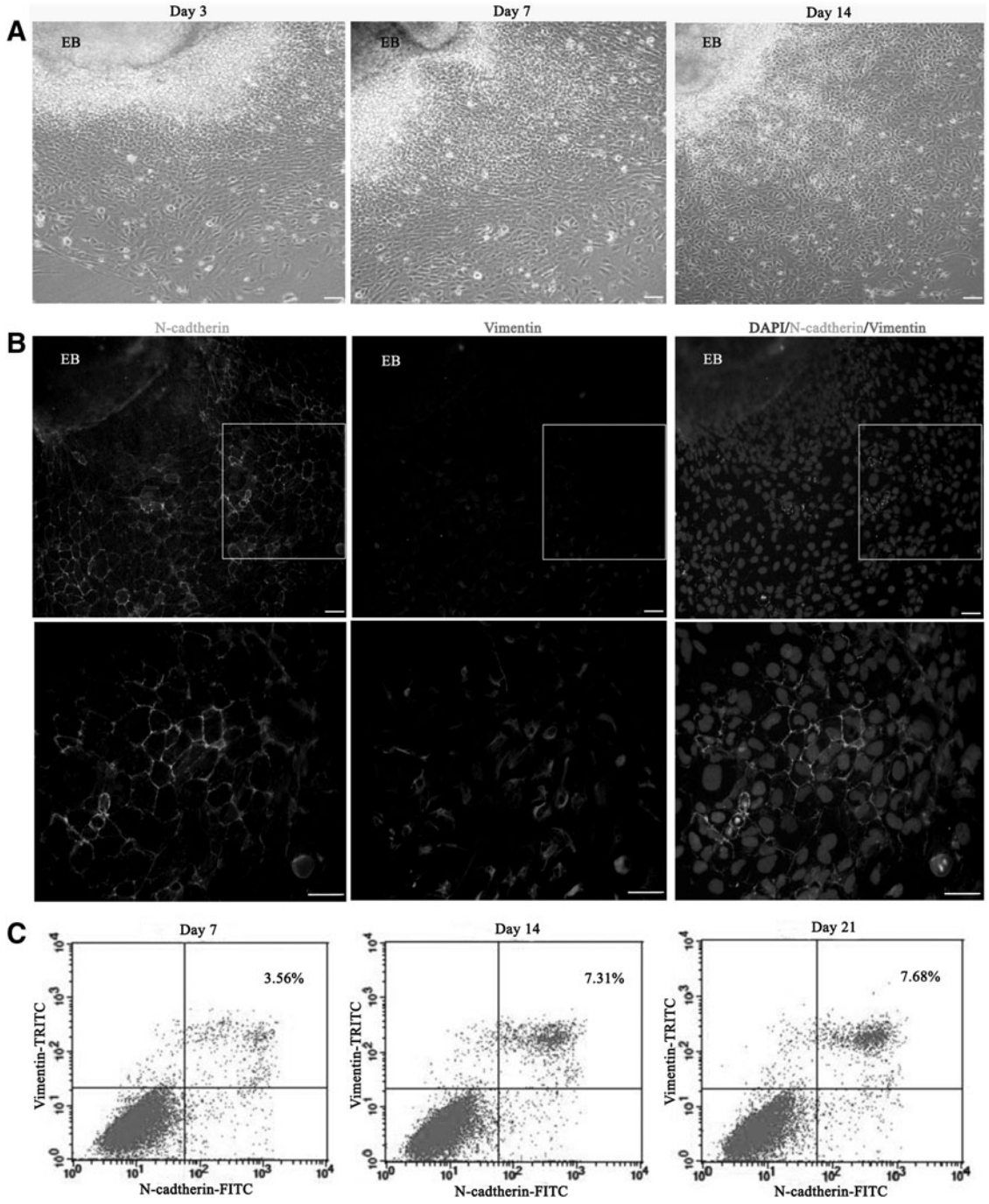

FIG. 2. Induction of putative human corneal endothelial cells (hCECs) from POMPs. **(A)** Morphological changes of POMPs after exposure to the CEC differentiation medium (EM) for further induction over 2 weeks. **(B)** Immunostaining of the plated EBs and POMPs after 14 days of exposure to EM. Coexpression of N-cadherin and vimentin was found in putative hCECs. The pictures at the *bottom* are higher magnifications of differentiated POMPs. **(C)** Analysis of N-cadherin/vimentin dual-positive cells by FACS. The mean proportion of dual-positive cells was about 3.56% 7 days after induction and increased to 7.31% on day 14, whereas there was no increase from 14 to 21 days. The *dot plots* are representative of three independent experiments. Scale bars = 20 μm.

extended to 10 days, the cell density did not continue to increase, indicating the existence of cell-to-cell contact inhibition. In addition, the proliferation potential of CEC-like cells was extremely limited, which was proved by the fact that these cells can be cultured only within one to two passages. These biological features of CEC-like cells were similar to normal human CECs. Immunofluorescent results demonstrated that positive signals for Na^+/K^+ ATPase α1 and ZO-1 were detected throughout the membrane of CEC-like cells (Fig. 3B, DAPI/ZO-1, DAPI/Na^+/K^+ ATPase α1). Additionally, the expanded CEC-like cells still expressed N-cadherin and vimentin (Fig. 3B, DAPI/vimentin, DAPI/N-cadherin), indicating that the characteristics of these cells were maintained under current culture

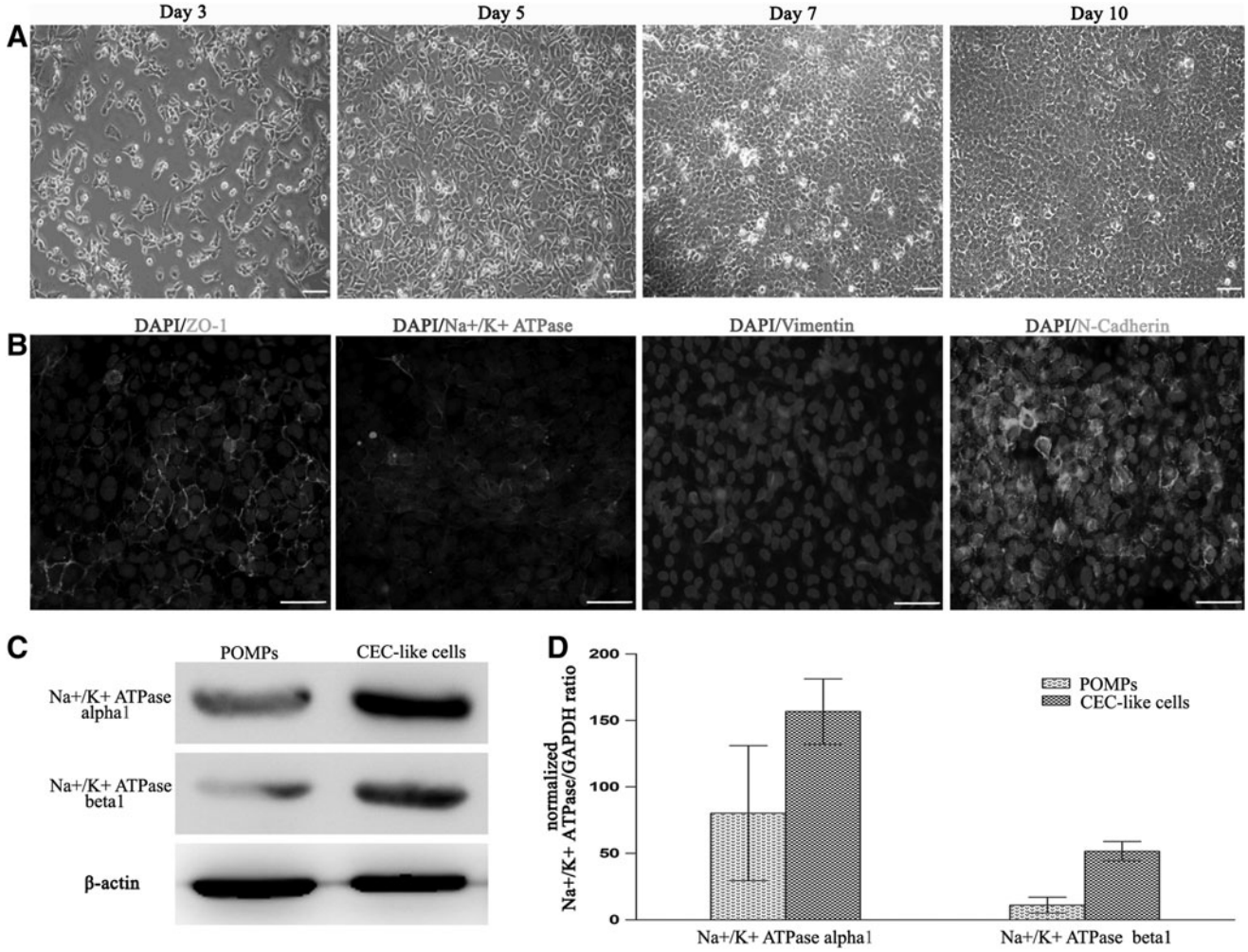

FIG. 3. Characterization of the isolated CEC-like cells after culturing two passages and the expression of Na^+/K^+ ATPase α1 and β1 subunits in POMPs and CEC-like cells. **(A)** CEC-like cells displayed a hexagonal and pentagonal shape and grown to form a monolayer of cells, characteristic of morphology of normal human corneal endothelium (CE). **(B)** Positive signals for zonula occludens-1 (ZO-1), Na^+/K^+ ATPase, and N-cadherin were detected throughout the cytomembrane and positive signals for vimentin were distributed in the cell plasma. **(C)** Western blotting showed that the expression of sodium-potassium pump Na^+/K^+ ATPase (α1 and β1 subunits), an important CEC-related functional protein, was higher in CEC-like cells than that in POMPs. The loading variation was shown by β-actin. **(D)** Real-time reverse transcription–polymerase chain reaction indicated that the expression of Na^+/K^+ ATPase α1 and β1 subunit gene was upregulated in the differentiated POMPs (ie, CEC-like cells). Scale bars = 20 μm.

conditions. Although just-mentioned results demonstrated that the biological features and function-related protein profile of CEC-like cells were consistent with native human CECs [42,43], the evidence for the ability to maintain stroma dehydration was indispensable because it was the gold standard for identification of CECs. To evaluate the pump function of CEC-like cells, the CEC-like cell sheet was constructed.

Characterization of PAPCM lamellae and CEC-like cell sheets

The PAPCM lamella was opaque after the process of decellularization on gross observation (Fig. 4A). But its transparency was restored after soaking in sterile glycerol for 1 h (Fig. 4B). H&E staining showed that no visible cells or nuclear material was observed in the PAPCM lamella, while collagen fibers and Descemet's membrane were retained and had normal structure (Fig. 4C).

The CEC-like cell sheet was efficiently constructed with CEC-like cells and PAPCM lamella. The CEC-like cells were labeled with CFDA SE before seeding on the PAPCM lamella. After 2 weeks of seeding, CFDA SE-positive signals were observed on the surface of Descemet's membrane (Fig. 4D). The clear outline of CFDA SE-positive CEC-like cells was markedly delineated by dual staining with trypan blue and alizarin S, appearing as nearly confluent packed hexagonal and pentagonal morphology compatible with human CEC identity (Fig. 4E). The mean cell density of CEC-like cell sheet was $3{,}580 \pm 223$ cells/mm^2 (ranged from 3,210 to 3,950 cells/mm^2, $n = 30$). H&E staining showed that CEC-like cells formed an almost intact monolayer on the surface of Descemet's membrane and no cells were discovered within the PAPCM lamella (Fig. 4F).

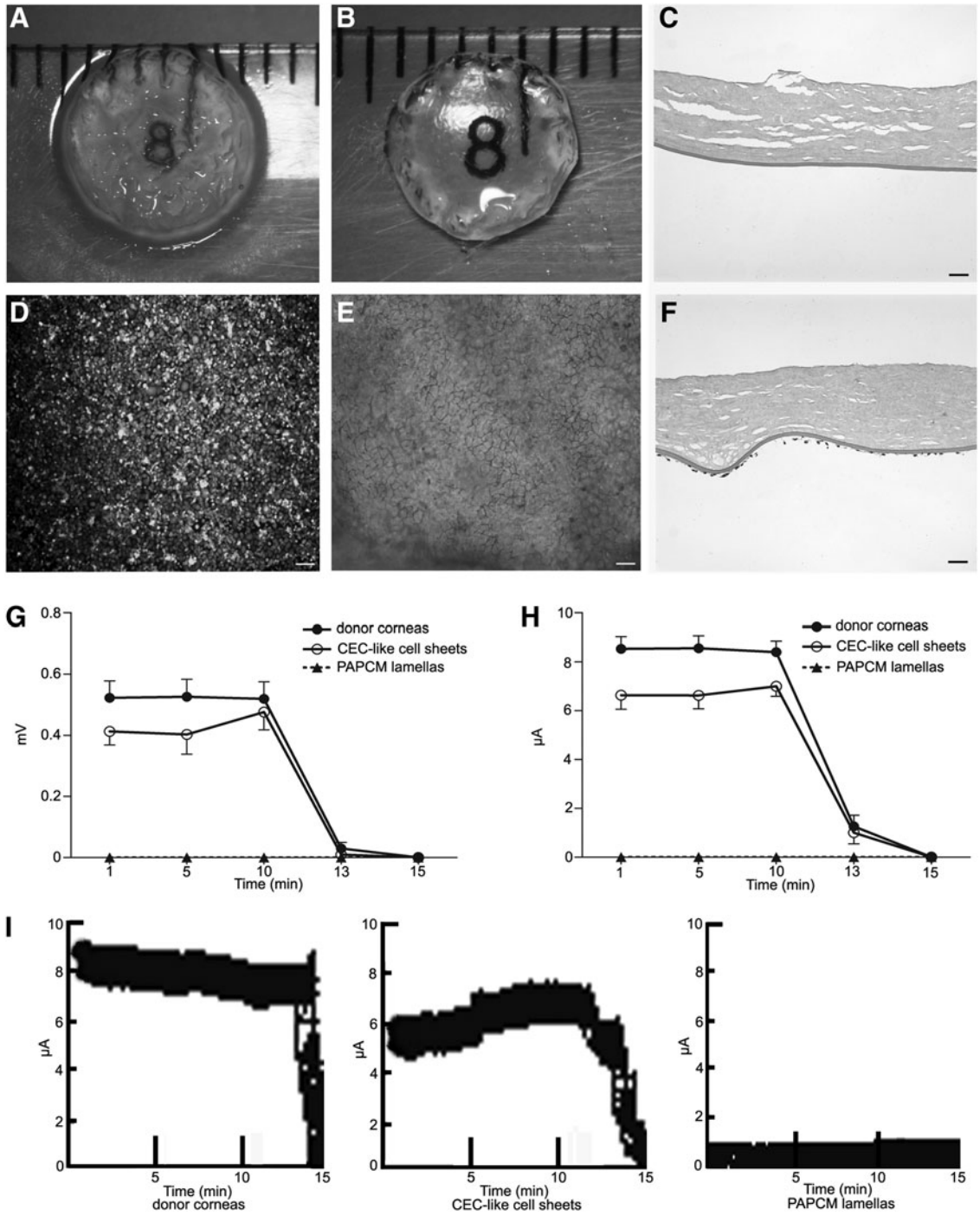

FIG. 4. Characteristics of the posterior acellular porcine corneal matrix (PAPCM) lamella and the CEC-like cell sheet. **(A)** The PAPCM lamella was opaque due to the process of decellularization on gross observation. **(B)** The PAPCM lamella became transparent when soaked in 100% sterile glycerol. **(C)** Hematoxylin and eosin (H&E) staining showed that the PAPCM lamella was cell free. **(D)** Carboxyfluorescein diacetate, succinimidyl ester (CFDA SE)–positive signals were observed on the surface of CEC-like cell sheet. **(E)** Alizarin red S and trypan blue double staining of the CEC-like cell sheet showed the ''lake reaction'' of cell borders and no multiple layers from plane view. **(F)** H&E staining of the CEC-like cell sheet showed that CEC-like cells kept a monolayer on Descemet's membrane in cross-sectional view. **(G, H)** Time course changes in the potential differences and short-circuit current in a CEC-like cell sheet. **(I)** Raw data of current tracings. Data shown are for (●) human epithelium-deprived donor corneas, (○) CEC-like cell sheets, and (▲) PAPCM lamellae; $n = 3$ in each group. Data are the mean ± SD. Scale bars = 20 μm.

Evaluation of pump function of CEC-like cells in vitro

Time-course changes in the average and standard deviations of the potential differences and short-circuit current in the donor corneas, CEC-like cell sheets, and PAPCM lamellae are shown in Fig. 4. Average potential differences in the CEC-like cell sheets at 1, 5, and 10 min were 79%, 77%, and 92% of the value for human donor corneas deprived of epithelium (Fig. 4G) and the average short-circuit current was 78%, 77%, and 83% of it at the same time point (Fig. 4H). The potential differences and average short-circuit current for the APCMPL sheets and for human donor corneas deprived of the epithelium and endothelium (data not shown) were 0 at each time point. After the Na^+/K^+ ATPase inhibitor ouabain was added to the chambers, the potential differences and average short-circuit current became 0 in all the specimens within 5 min. Figure 4I was representative of raw data of current tracings.

These findings suggested that hESC-derived CEC-like cells had adequate transport activity, similar to normal human CECs. Next we evaluated the pump function of CEC-like cells in vivo.

Stripping rabbit central corneal Descemet's membrane and replacing it with CEC-like cell sheet

The Figure 5 shows the whole steps of the operation in which first the corneal surface was marked using a trephine with a diameter of 7.5 mm and a circle trace was clearly observed (Fig. 5A) and then the Descemet's membrane was spitted in circumference along the circle trace with a sharp hook (Fig. 5B) and separated from the stroma bluntly (Fig. 5C); at last, the isolated Descemet's membrane was removed from the anterior chamber of the eye (Fig. 5D). Subsequently, a 8.0-mm-diameter CEC-like sheet or PAPCM lamella was folded by forceps, Descemet's membrane side in, and inserted into the anterior chamber (Fig. 5F). For CEC-like cell sheet, 0.1 mL of sodium chondroitin sulfate–sodium hyaluronate was dropped on the surface of Descemet's membrane before it was inserted into the anterior chamber, in order to protect the CEC-like cells from damage due to mechanic manipulation and induce the loss of CEC-like cells (Fig. 5E). Then, the folded sheet was spread out with Descemet's membrane facing the anterior chamber (Fig. 5G), and adhered to the recipient stroma by injecting a sterile air bubble into the anterior chamber (Fig. 5H).

Clinical observations

Pump function of CEC-like cells in vivo was investigated by clinical observations in a rabbit model having borne the surgical operation (Fig. 5). Representative anterior segment photographs of a slit-lamp biomicroscope and visante OCT were shown in Fig. 6 on postoperative days 3, 7, 14, and 28, respectively. It was obvious that the corneal transparency was increased gradually and almost completely restored in the CEC-like cell group 28 days after surgery (Fig. 6A), whereas the degree of corneal opacity and stromal edema was more and more aggravated in the PAPCM lamellae group (Fig. 6B). No apparent inflammatory reactions suggesting immune rejection were observed using a slit-lamp microscope during follow-up period. Corneal thickness is an important parameter for evaluating CEC function. As shown in Fig. 6C, the corneal thickness increased consistently throughout the 28-day observation period in the PAPCM lamellae group. In contrast, mean corneal thickness in the CEC-like cell group gradually decreased, becoming

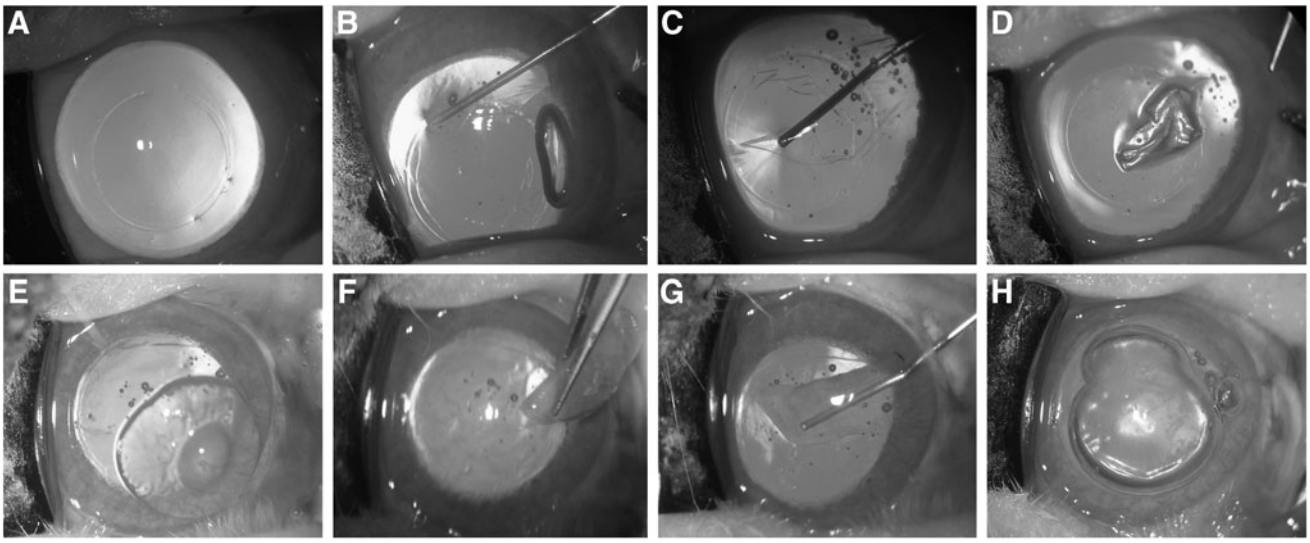

FIG. 5. Surgical procedure for the CEC-like cell sheet transplantation. **(A)** A diameter of 7.5-mm circle trace marker was made on the central rabbit corneal surface using a trephine. **(B, C)** The Descemet's membrane was spitted in circumference along the circle trace with a sharp hook **(B)** and separated from the stroma bluntly **(C)**. **(D)** The isolated Descemet's membrane was removed from the anterior chamber of the eye. **(E)** The surface of Descemet's membrane of the CEC-like cell sheet was coated with an ophthalmic viscosurgical device. **(F)** The sheet was folded and inserted into the anterior chamber. **(G)** The folded sheet was spread out in the anterior chamber. **(H)** The sheet was attached to the posterior stroma by injecting a sterile air bubble into the anterior chamber.

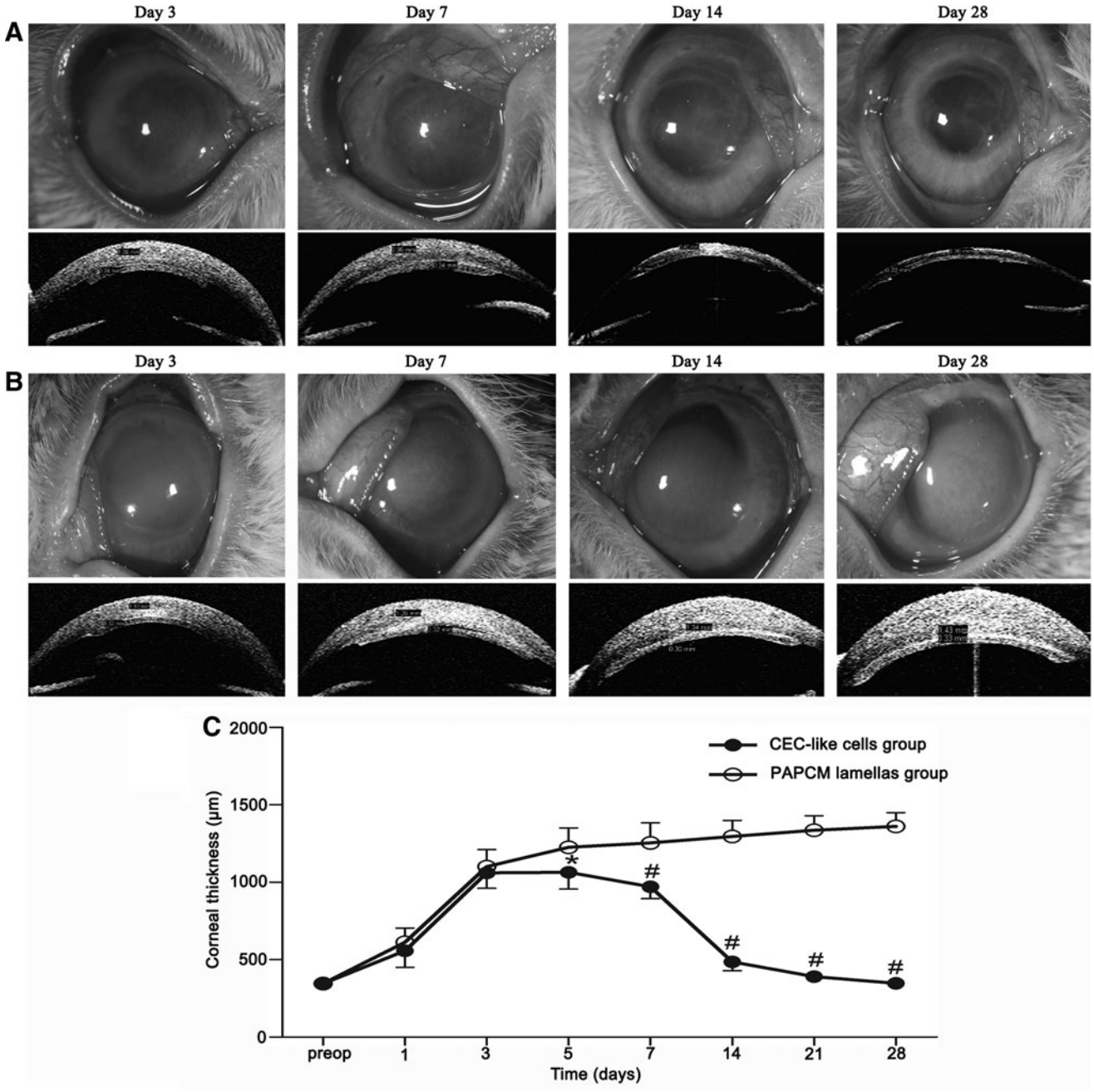

FIG. 6. Observations after the surgery. **(A, B)** Representative anterior segment photographs made with a slit-lamp microscope (the *top row*) and visante OCT (the *bottom row*) at different time points. **(A)** The corneal transparency was restored and stromal edema disappeared gradually in the CEC-like cell group. **(B)** The degree of corneal opacity and stromal edema was more and more aggravated in the PAPCM lamellae group. **(C)** Changes of corneal thickness during clinical observation. There are significant differences in corneal thickness ($^{*}P < 0.05$, $^{\#}P < 0.001$) between the PAPCM lamellae (○) and CEC-like cell group (●) on days 5, 7, 14, 21, and 28. Error bars = SD.

significantly less than that in the PAPCM lamellae group 5 ($P < 0.05$), 7, 14, 21, and 28 days ($P < 0.0001$) after surgery.

Evaluation of CEC-like cells in the rabbit model and histological examination

Representative specular microscope images confirmed full coverage of the Descemet's membrane by polygonal cells in the CEC-like cell group and the cell density was $2{,}738 \pm 221$ cells/mm^2 28 days after surgery (Fig. 7A), whereas preoperative density was $3{,}580 \pm 223$ cells/mm^2. In contrast the details of Descemet's membrane surface could not be described with a specular microscope in the PAPCM lamellae group because the corneas were opaque and transmitting of light was extremely limited. Then, confocal microscopy through focusing was used to examine PAPCM lamellae group corneas. The confocal microscope image showed that the Descemet's membrane of the central cornea

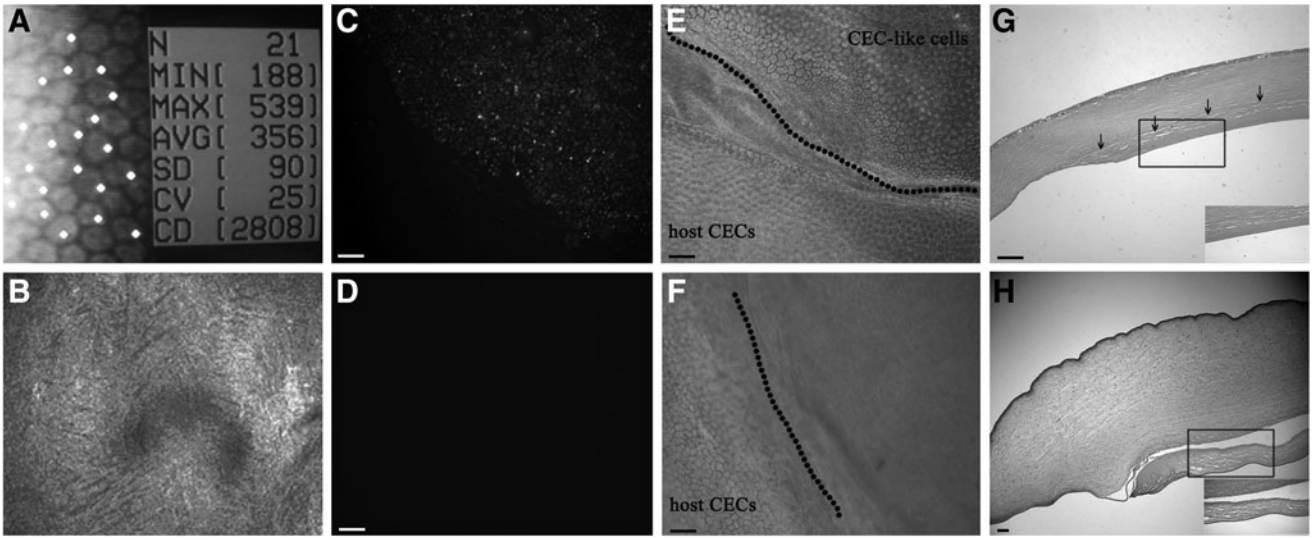

FIG. 7. Evaluation of CEC-like cells localizing on the posterior surface of corneas and histological examination of corneas in the rabbit model. **(A)** Specular microscope confirmed the polygonal cell coverage of the Descemet's membrane in the CEC-like cell group. **(B)** There was only denuded Descemet's membrane in the PAPCM lamellae group. **(C–F)** Trypan blue and alizarin S costaining and fluorescence microscopy examination of whole-mount corneas. CFDA SE-positive cells were observed in the CEC-like cell group **(C)**, while there were no signals checked in the PAPCM lamellae group **(D)**. Trypan blue and alizarin S costaining showed that CEC-like cells were alive and clearly delineated the cell boundaries in the CEC-like cell group **(E)**, whereas the staining was negative on the surface of PAPCM lamella in the PAPCM lamellae group **(F)**. **(G)** H&E staining showed the integration of sheet with recipient cornea and a CEC-like cell monolayer present on the surface in the CEC-like cell group. **(H)** In the PAPCM lamellae group, the cornea was edema and the PAPCM lamella was detached from recipient cornea. *Insets* in **(G, H)** are higher magnifications. Scale bars = 20 μm.

was denuded and no cells were detected in PAPCM lamellae group (Fig. 7B). Unlike humans, the rabbit CECs have the capacity of self-renewal and the lost cells due to disease or injury can be complemented by regeneration [44]. The microscope provided the morphology of corneal endothelia in vivo and indicated that there was no obvious regeneration of residual host CECs during the 28-day observation period in the PAPCM lamellae group. To explore the origin of polygonal cells in CEC-like cell group, the signal for CFDA SE was checked and the results showed that it was positive in this group (Fig. 7C), indicating their origin from transplanted CEC-like cells but not host CECs. As negative control, there were no signals observed in the PAPCM lamellae group (Fig. 7D). The corneal transparency was restored gradually in the CEC-like cell group (Fig. 6A), indicating the existence of enough normal CECs. To further investigate the survival of CEC-like cells, trypan blue and alizarin S costaining, a simple and quick technique for visualization of both damaged and normal CECs, was performed in vitro on postoperative day 28. The quasiregular forms with well-defined cell boundaries were clearly visible (Fig. 7E) in the CEC-like cell group, whereas the staining was negative on the surface of PAPCM lamella in the PAPCM lamellae group (Fig. 7F), indicating that the polygonal cells in the CEC-like cell group were normal CECs. Therefore, it was concluded that the cells covering the inner surface of central corneas in the CEC-like cell group were composed of normal CEC-like cells.

In addition H&E staining was performed on day 28 post-transplantation. The results showed that the CEC-like cell sheet integrated with the recipient cornea and a CEC-like cell monolayer localized on the surface of the sheet in the CEC-like cell group (Fig. 7G). In contrast, in the PAPCM lamellae group, severe stromal edema and detachment of PAPCM lamella from the posterior surface of the recipient cornea was observed and no cells were detected on the surface of PAPCM lamella (Fig. 7H). There was no evidence of mononuclear cell accumulation or neoplasm occurring in the two groups, suggesting the excellent biocompatibility and safety both of CEC-like cells and PAPCM lamellae.

Discussion

It has been demonstrated that in vivo, majority of anterior eye segment structures, including CE, develop from populations of POMPs in mammals and other vertebrates [12]. Fate maps developed in birds demonstrated that POMPs arise developmentally from both neural crest and mesoderm and further established that the CECs are derived solely from the neural-crest-derived POMPs [45,46]. However, there are important differences between birds and mammals. In mammals, most CECs are derived from the neural crest while a small population of CECs originates from mesoderm [12]. To date, the specific origination of human CECs has yet not to be determined. In this study, we went through an intermediate phase of the derivation of POMPs from hESCs during the process of hESCs differentiating into CECs. However, we could not distinguish neural crest or mesoderm origination of the hESC-derived POMPs due to the lack of special markers. Previous studies demonstrated the feasibility of generating CEC-like cells both from rat neural crest

cells and mesoderm-derived human UCB-MSCs [28,35]. Therefore we assume that human CECs may receive initial contributions from both neural crest and mesoderm during human eye development, similar to that of mammals. In future study, searching for molecular markers that distinguish POMPs of mesoderm and neural crest derivation in our coculture system would be possible solution to illuminate the initial origin of human CECs.

The mesenchymal precursor marker CD73 was found in the spindle-like cells emigrating from hESC-derived EBs when cocultured with differentiated hCSCs and the numbers of CD73-positive cells peaked around day 5 as evidenced by FACS, indicating POMPs began to spontaneously differentiate into some terminal cell lineages on the 5th day. Although these terminal differentiated cell types were not further investigated, the cell morphology indicated no obvious occurrence of CEC-like cells under FM culture medium (data not shown). Hence, the culture medium was changed from FM to EM on day 5 in order to direct the POMPs to differentiate toward CEC-like cells. In addition, hCSCs could not reach complete confluence on day 5 and the induction efficiency would not be compromised using transwell coculture system to differentiate hESCs into POMPs, since cell confluence might clog the porous membrane in the top chamber resulting in inefficient leaking of cytokines into the bottom chamber [47]. In the same way, this is the reason why the conditioned medium was used to induce CEC-like cells from POMPs instead of transwell coculture system because the time needed for CEC-like cell induction was far beyond that for lens epithelial cell confluence. According to previous studies, conditioned medium should be collected when the cells are in their best state and properly stored to save their biological activity. In this study, LECCM was collected when lens epithelial cells reached about 70%–90% confluence, every 12 h after medium change, and filtered LECCM was stored at $-20°C$ as suggested.

In vivo, cell shape and the ability of cells to maintain corneal transparency are major criteria for identification of healthy CE. In vitro identification of CECs is problematic since authentic phenotypic markers for CECs have not been identified. Due to this reason, a combination of criteria was used for CEC identification in our study. These include cell shape, the expression of several CEC differentiation and function-related proteins and transcription factors, as well as the curative effect of animal transplantation. The alteration of cell shape; the upregulation of Na^+/K^+ ATPase α and β subunits; the positive expression of N-cadherin, vimentin, FoxC1, Pitx2, Na^+/K^+ ATPase, and ZO-1; and the clinical observations after transplantation into rabbit models demonstrated that the POMPs differentiated toward CECs under EM conditions and the differentiated POMPs had properties similar to those of native CECs. It is worth mentioning that the isolated N-cadherin/vimentin dual-positive CEC-like cells still expressed N-cadherin and vimentin after culturing two passages, indicating that the characteristics of these cells remained unchanged. However, whether the biological characteristics are still unaltered after more passages is unknown, because the proliferation capacity of CEC-like cells is limited under current culture conditions. How to achieve the massive amplification of CEC-like cells and meanwhile maintain their characteristics is the issue of interest. In addition our results showed that the shape of POMPs was modified to extremely resemble that of native CECs while previous study indicated that the shape of human UCB-MSCs was similar to that of lens fiber cells when incubated in the same medium. Given the fact that the components of conditioned medium are similar, we propose that the differences in cell morphology are due to cell-intrinsic differences between POMPs and UCB-MSCs rather than an artifact of in vitro culture. Combining the fact that UCB-MSCs are derived from paraxial mesoderm, we suggest that POMPs may predominantly consist of precursors of neural crest origin. Of course, further experiments are needed for the final conclusion.

At present, very little is known about the molecular mechanism that regulates the development of CE. The existing literatures have demonstrated that transforming growth factor-β2 (TGF-β2) is closely related to CE development [38]. TGF-β2 functions as the major signaling ligand of POMPs to control the normal expression of transcription factor genes of FoxC1 and Pitx2 that are vital for the development of CE. Ablation of TGF-β2 results in the loss of expression of FoxC1 and Pitx2 in POMPs and agenesis of CE. Another potential candidate that is closely related to CE development is retinoic acid (RA). Previous studies have indicated that ablation of RA signaling leads to agenesis of CE with associated loss of anterior chamber and thinning of corneal stroma, features that are similar to TGF-β2 signaling blocking mutants [48]. The differentiation medium used in this study is a mixture composed of many kinds of ingredients secreted from hCSCs and LECs, including TGF-β2 and RA. Therefore, it is our interest to determine not only whether RA and TGF-β2 signaling act in concert or independently in CEC-like cells induction but also the underlying mechanism(s) and to identify the existence of other molecular signals and their potential relationship to RA and TGF-β2 signaling. Further investigation concerning the identification of species of these secreted factors and scenarios of their temporal expression is needed to achieve this goal and optimize the differentiation protocol to improve the inductivity of CECs from hESCs in the future.

To evaluate the pump function of CEC-like cells and the potential of them in regenerative medicine, we constructed the CEC-like cell sheets and performed the transport activity assay in vitro and the animal transplantation experiments in vivo. We found that the potential differences and short-circuit current of a CEC-like cell sheet were similar to those of donor corneas, suggesting that the pump function was satisfactory in reconstructed CEC-like cell sheets. Rabbit corneas receiving CEC-like cell sheets showed decreased corneal edema, whereas severe stromal edema was present throughout the follow-up period in corneas receiving PAPCM lamellae. The transplanted CEC-like cells by means of a PAPCM lamella survived in majority and contributed to restoration of corneal transparency in the rabbit CE dysfunction models. It is an exciting fact that no immune rejection occurred in this human/pig-to-rabbit xenotransplantation model during 28-day observation period, while in the full-thickness murine corneal xenotransplantation model corneal xenografts were rejected over a period of 2–16 days after transplantation [49–51]. The characteristic of anterior chamber of the eye, being an immune-privileged site and equipped with anterior-chamber-associated immune

deviation (ACAID), permits the long-term acceptance and survival of histoincompatible tissue grafts [52,53]. Additionally hESC-derived cells expressed only moderate amounts of MHC class I and not any MHC class II proteins; therefore, hESC-derived cells had weak immunogenicity [54]. In CEC-like cell sheet transplantation, the transplanted CEC-like cells that face the anterior chamber may induce ACAID and these cells were derived from hESCs, thereby avoiding immune rejection. In addition, it has been demonstrated that keratocytes were important targets during xenograft rejection [55,56] and the decellularization procedure increased pig corneal graft survival in pig-to-rhesus lamellar corneal xenotransplantation [57]. In this study, as shown in representative H&E staining of PAPCM lamellae (Fig. 4C), the cell components had been completely removed. Therefore, it is acceptable that there were no signs of immune rejection detected either in PAPCM lamellae or CEC-like cell sheet transplantation. However, we cannot rule out the possibility of the existence of mild subclinical immune rejection because postoperative endothelial cell density on the CEC-like cell sheets decreased compared with preoperative density, which meant that small number of CEC-like cells may be swallowed by the rabbit phagocytic cells during our observation period. In addition the observation period was limited. Therefore, the further investigation was needed. The restoration of corneal transparency and no notable episode of acute immune rejection in the CEC-like cell group indicated that the reconstructed CEC-like cell sheet may be a promising substitute for a human corneal allograft for treatment of human CE dysfunction in the future.

In summary, POMPs could be generated by coculturing hESCs with differentiated hCSCs. LECCM from human lens epithelial cells could induce these POMPs to differentiate into functional CEC-like cells. The derivation of CEC-like cells from hESCs via POMP phase recapitulated the development pattern of mammal CECs in vivo and provided the evidence that human CECs also originate from POMPs like other vertebrate species. In addition, our findings indicated that transplantation of CEC-like cells by means of a PAPCM lamellae can retain their function of corneal dehydration and restore the transparency of cornea in a rabbit CE dysfunction model. Thus, hESCs represent a renewable source of human CECs that can be readily and rapidly accessed for studies of both normal and disordered human CEC development and potential applications in human CE dysfunction management in the future.

Acknowledgments

The authors thank the Center of Reproductive Medicine, Shandong University, for providing hESCs and its staff member Dr. Sexin Huang for technical support in culturing the cells. The authors also thank Dr. Edward C. Mignot, formerly of Shandong University, for linguistic advice. This work was supported by grants from the National Natural Science Fund of China (81271716) and the Key Scientific and Technological Project of Shandong Province, People's Republic of China (2008GGB02111).

Author Disclosure Statement

No competing financial interests exist.

References

1. Thomson JA, J Itskovitz-Eldor, SS Shapiro, MA Waknitz, JJ Swiergiel, VS Marshall and JM Jones. (1998). Embryonic stem cell lines derived from human blastocysts. Science 282:1145–1147.
2. Reubinoff BE, MF Pera, CY Fong, A Trounson and A Bongso. (2000). Embryonic stem cell lines from human blastocysts: somatic differentiation in vitro. Nat Biotechnol 18:399–404.
3. Reubinoff BE, P Itsykson, T Turetsky, MF Pera, E Reinhartz, A Itzik and T Ben-Hur. (2001). Neural progenitors from human embryonic stem cells. Nat Biotechnol 19:1134–1140.
4. Zhang SC, M Wernig, ID Duncan, O Brüstle and JA Thomson. (2001). In vitro differentiation of transplantable neural precursors from human embryonic stem cells. Nat Biotechnol 19:1129–1133.
5. Perrier AL, V Tabar, T Barberi, ME Rubio, J Bruses, N Topf, NL Harrison and L Studer. (2004). Derivation of midbrain dopamine neurons from human embryonic stem cells. Proc Natl Acad Sci U S A 101:12543–12548.
6. Li XJ, ZW Du, ED Zarnowska, M Pankratz, LO Hansen, RA Pearce and SC Zhang. (2005). Specification of motoneurons from human embryonic stem cells. Nat Biotechnol 23:215–221.
7. Lee H, GA Shamy, Y Elkabetz, CM Schofield, NL Harrsion, G Panagiotakos, ND Socci, V Tabar and L Studer. (2007). Directed differentiation and transplantation of human embryonic stem cell derived motoneurons. Stem Cells 25:1931–1939.
8. Sottile V, A Thomson and J McWhir. (2003). In vitro osteogenic differentiation of human ES cells. Cloning Stem Cells 5:149–155.
9. Barberi T, LM Willis, ND Socci and L Studer. (2005). Derivation of multipotent mesenchymal precursors from human embryonic stem cells. PLoS Med 2:0554–0560.
10. Karp JM, LS Ferreira, A Khademhosseini, AH Kwon, J Yeh and RS Langer. (2006). Cultivation of human embryonic stem cells without the embryoid body step enhances osteogenesis in vitro. Stem Cells 24:835–843.
11. Brown SE, W Tong and PH Krebsbach. (2009). The derivation of mesenchymal stem cells from human embryonic stem cells. Cells Tissues Organs 189:256–260.
12. Gage PJ, W Rhoades, SK Prucka and T Hjalt. (2005). Fate maps of neural crest and mesoderm in the mammalian eye. Invest Ophthalmol Vis Sci 46:4200–4208.
13. Murphy C, J Alvarado, R Juster and M Maglio. (1984). Prenatal and postnatal cellularity of the human corneal endothelium. A quantitative histologic study. Invest Ophthalmol Vis Sci 25:312–322.
14. Bourne WM, LR Nelson and DO Hodge. (1997). Central corneal endothelial cell changes over a ten-year period. Invest Ophthalmol Vis Sci 38:779–782.
15. Hollingsworth J, I Perez-Gomez, HA Mutalib and N Efron. (2001). A population study of the normal cornea using an in vivo, slit-scanning confocal microscope. Optom Vis Sci 78:706–711.
16. Joyce NC, DL Harris and DM Mello. (2002). Mechanisms of mitotic inhibition in corneal endothelium: contact inhibition and TGF-beta2. Invest Ophthalmol Vis Sci 43:2152–2159.
17. Rosenbaum K, J Rottler, R Steinbach and KK Huber. (2010). Reduced availability of potential cornea donors: reasons and suggestions. Klin Monatsbl Augenheilkd 227: 418–422.

18. Huan Q, X Gao, Y Wang, Y Shen, W Ma and ZJ Chen. (2010). Comparative evaluation of human embryonic stem cell lines derived from zygotes with normal and abnormal pronuclei. Dev Dyn 239:425–438.
19. Du L, X Wu, K Pang and Y Yang. (2011). Histological evaluation and biomechanical characterisation of an acellular porcine cornea scaffold. Br J Ophthalmol 95:410–414.
20. Pang K, L Du and X Wu. (2010). A rabbit anterior cornea replacement derived from acellular porcine cornea matrix, epithelial cells and keratocytes. Biomaterials 31:7257–7265.
21. Wigham C and S Hodson. (1981). The effect of bicarbonate ion concentration on trans-endothelial short circuit current in ox corneas. Curr Eye Res 1:37–41.
22. Wigham CG, HC Turner, J Swan and SA Hodson. (2002). Modulation of corneal endothelial hydration control mechanisms by Rolipram. Pflugers Arch 440:866–870.
23. Tanaka T. (2000). Comparison of stromal remodeling and keratocyte response after corneal incision and photorefractive keratectomy. Jpn J Ophthalmol 44:579–590.
24. Uchida S, S Yokoo, Y Yanagi, T Usui, C Yokota, T Mimura, M Araie, S Yamagami and S Amano. (2005). Sphere formation and expression of neural proteins by human corneal stromal cells in vitro. Invest Ophthalmol Vis Sci 46:1620–1625.
25. Draper JS, C Pigott, JA Thomson and PW Andrews. (2002). Surface antigens of human embryonic stem cells: changes upon differentiation in culture. J Anat 200:249–258.
26. Perris R and D Perissinotto. (2000). Role of the extracellular matrix during neural crest cell migration. Mech Dev 95:3–21.
27. Blake DA, H Yu, DL Young and DR Caldwell. (1997). Matrix stimulates the proliferation of human corneal endothelial cells in culture. Invest Ophthalmol Vis Sci 38: 1119–1129.
28. Ju C, K Zhang and X Wu. (2012). Derivation of corneal endothelial cell-like cells from rat neural crest cells in vitro. PLoS One 7:1–10.
29. Iwao K, M Inatani, Y Matsumoto, M Ogata-Iwao, Y Takihara, F Irie, Y Yamaguchi, S Okinami and H Tanihara. (2009). Heparan sulfate deficiency leads to Peters anomaly in mice by disturbing neural crest TGF-β2 signaling. J Clin Invest 119:1997–2008.
30. Coulombre AJ and JL Coulombre. (1964). Lens development. I. Role of the lens in eye growth. J Exp Zool 156:39–47.
31. Genis-Galvez JM. (1966). Role of the lens in the morphogenesis of the iris and cornea. Nature 210:209–210.
32. Zinn KM. (1970). Changes in corneal ultrastructure resulting from early lens removal in the developing chick embryo. Invest Ophthalmol 9:165–182.
33. Beebe DC and JM Coats. (2000). The lens organizes the anterior segment: specification of neural crest cell differentiation in the avian eye. Dev Biol 220:424–431.
34. Zhang Y, PA Overbeek and V Govindarajan. (2007). Perinatal ablation of the mouse lens causes multiple anterior chamber defects. Mol Vis 13:2289–2300.
35. Joyce NC, DL Harris, V Markov, Z Zhang and B Saitta. (2012). Potential of human umbilical cord blood mesenchymal stem cells to heal damaged corneal endothelium. Mol Vis 18:547–564.
36. Alward WL. (2000). Axenfeld-Rieger syndrome in the age of molecular genetics. Am J Ophthalmol 130:107–115.
37. Kume T, KY Deng, V Winfrey, DB Gould, MA Walter and BL Hogan. (1998). The forkhead/winged helix gene Mf1 is disrupted in the pleiotropic mouse mutation congenital hydrocephalus. Cell 93:985–996.
38. Ittner LM, H Wurdak, K Schwerdtfeger, T Kunz, F Ille, P Leveen, TA Hjalt, U Suter, S Karlsson, et al. (2005). Compound developmental eye disorders following inactivation of TGF-β signaling in neural-crest stem cells. J Biol 4:1–16.
39. Holmberg J, CY Liu and TA Hjalt. (2004). PITX2 gain-of-function in Rieger syndrome eye model. Am J Pathol 165:1633–1641.
40. Reneker LW, DW Silversides, L Xu and PA Overbeek. (2000). Formation of corneal endothelium is essential for anterior segment development—a transgenic mouse model of anterior segment dysgenesis. Development 127:533–542.
41. Risen LA, PS Binder and SK Noyok. (1987). Intermediate filaments and their organization in human corneal endothelium. Inves Ophthalmol Vis Sci 28:1933–1938.
42. Joyce NC and CC Zhu. (2004). Human corneal endothelial cell proliferation: potential for use in regenerative medicine. Cornea 23(8 Suppl):S8–S19.
43. Joyce NC. (2005). Cell cycle status in human corneal endothelium. Exp Eye Res 81:629–638.
44. Van Horn DL, DD Sendele, S Seideman and PJ Buco. (1997). Regenerative capacity of the corneal endothelium in rabbit and cat. Invest Ophthalmol Vis Sci 16:597–613.
45. Johnston MC, DM Noden, RD Hazelton, JL Coulombre and AJ Coulombre. (1979). Origins of avian ocular and periocular tissues. Exp Eye Res 29:27–43.
46. Le Lièvre CS and NM Le Douarin. (1975). Mesenchymal derivatives of the neural crest: analysis of chimaeric quail and chick embryos. J Embryol Exp Morphol 34:125–154.
47. Tian H, S Bharadwaj, Y Liu, PX Ma, A Atala and Y Zhang. (2010). Differentiation of human bone marrow mesenchymal stem cells into bladder cells: potential for urological tissue engineering. Tissue Eng Part A 16:1769–1779.
48. Matt N, V Dupé, JM Garnier, C Dennefeld, P Chambon, M Mark and NB Ghyselinck. (2005). Retinoic acid-dependent eye morphogenesis is orchestrated by neural crest cells. Development 132:4789–4800
49. Ross JR, DN Howell and FP Sanfilippo. (1993). Characteristics of corneal xenograft rejection in a discordant species combination. Invest Ophthalmol Vis Sci 34:2469–2476.
50. Yamagami S, M Isobe, H Yamagami, J Hori and T Tsuru. (1997). Mechanism of concordant corneal xenograft rejection in mice: synergistic effects of anti-leukocyte function-associated antigen-1 monoclonal antibody and FK506. Transplantation 64:42–48.
51. Tanaka K, J Yamada and JW Streilein. (2000). Xenoreactive CD4+T cells and acute rejection of orthotopic guinea pig corneas in mice. Invest Ophthalmol Vis Sci 41:1827–1832.
52. Streilein JW and JY Niederkorn. (1981). Induction of anterior chamber-associated immune deviation requires an intact, functional spleen. J Exp Med 153:1058–1067.
53. Streilein JW, D Bradley, Y Sano and Y Sonoda. (1996). Immunosuppressive properties of tissues obtained from eyes with experimentally manipulated corneas. Invest Ophthalmol Vis Sci 37:413–424.
54. Drukker M, H Katchman, G Katz, S Even-Tov Friedman, E Shezen, E Hornstein, O Mandelboim, Y Reisner and N

Benvenisty. (2006). Human embryonic stem cells and their differentiated derivatives are less susceptible to immune rejection than adult cells. Stem Cells 24:221–229.
55. Oh JY, MK Kim, JH Ko, HJ Lee, CG Park, SJ Kim, WR Wee and JH Lee. (2009). Histological differences in full-thickness vs. lamellar corneal pig-to-rabbit xeno-transplantation. Vet Ophthalmol 12:78–82.
56. Kim MK, JY Oh, HI Lee, JH Ko, HJ Lee, JH Lee and WR Wee. (2008). Susceptibility of porcine keratocytes to immune-mediated damage in xeno-related rejection. Transplant Proc 40:564–569.
57. Choi HJ, MK Kim, HJ Lee, JH Ko, SH Jeong, JI Lee, BC Oh, HJ Kang and WR Wee. (2001). Efficacy of pig-to-rhesus lamellar corneal xenotransplantation. Invest Ophthalmol Vis Sci 52:6643–6650.

Address correspondence to:
Dr. Xinyi Wu
Department of Ophthalmology
Qilu Hospital
Shandong University
107#, Wenhua Xi Road
Jinan 250012
People's Republic of China

E-mail: xywu8868@163.com

Received for publication October 20, 2013
Accepted after revision February 4, 2014
Prepublished on Liebert Instant Online February 5, 2014